1-1-2006

Flexural behaviour of hybrid FRP-concrete-steel double skin tubular members

T Yu
Hong Kong Polytechnic University, taoy@uow.edu.au

Y L. Wong
Hong Kong Polytechnic University

J G. Teng
Hong Kong Polytechnic University

S L. Dong
Zhejiang University

E S.S Lam
Hong Kong Polytechnic University

Flexural behaviour of hybrid FRP-concrete-steel double skin tubular members

Abstract

This paper presents the results of an experimental study on the flexural behavior of a new type of hybrid FRP-concrete-steel member as well as results from a corresponding theoretical model based on the plane section assumption and the fiber element approach. This new type of hybrid member is in the form of a double-skin tube, composed of a steel inner tube and an FRP outer tube with a concrete infill between the two tubes, and may be employed as columns or beams. The parameters examined in this study include the section configuration, the concrete strength, and the thicknesses of the steel tube and the FRP tube, respectively. The results presented in this paper show that these hybrid beams have a very ductile response because the compressive concrete is confined by the FRP tube and the steel tube provides ductile longitudinal reinforcement. The beams' flexural response, including the flexural stiffness, ultimate load, and cracking, can be substantially improved by shifting the inner steel tube toward the tension zone or by providing FRP bars as additional longitudinal reinforcement. The predictions from the theoretical model are in reasonably close agreement with the test results. Differences between the test and predicted results arise from factors not considered in the theoretical model, including the existence of a strain gradient in the confined concrete, concentrations of cracks and the slips between the concrete and the two tubes; these are issues to be accounted for in the development of a more accurate model in the future.

Keywords

tubular, behaviour, flexural, skin, double, steel, concrete, frp, members, hybrid

Disciplines

Engineering | Science and Technology Studies

Publication Details

Yu, T., Wong, Y. L., Teng, J. G., Dong, S. L. & Lam, E. S.S. (2006). Flexural behaviour of hybrid FRP-concrete-steel double skin tubular members. Journal of Composites for Construction, 10 (5), 443-452.

Flexural Behavior of Hybrid FRP-Concrete-Steel Double-Skin Tubular Members

T. Yu[1]; Y. L. Wong[2]; J. G. Teng[3]; S. L. Dong[4]; and E. S. S. Lam[5]

Abstract: This paper presents the results of an experimental study on the flexural behavior of a new type of hybrid FRP-concrete-steel member as well as results from a corresponding theoretical model based on the plane section assumption and the fiber element approach. This new type of hybrid member is in the form of a double-skin tube, composed of a steel inner tube and an FRP outer tube with a concrete infill between the two tubes, and may be employed as columns or beams. The parameters examined in this study include the section configuration, the concrete strength, and the thicknesses of the steel tube and the FRP tube, respectively. The results presented in this paper show that these hybrid beams have a very ductile response because the compressive concrete is confined by the FRP tube and the steel tube provides ductile longitudinal reinforcement. The beams' flexural response, including the flexural stiffness, ultimate load, and cracking, can be substantially improved by shifting the inner steel tube toward the tension zone or by providing FRP bars as additional longitudinal reinforcement. The predictions from the theoretical model are in reasonably close agreement with the test results. Differences between the test and predicted results arise from factors not considered in the theoretical model, including the existence of a strain gradient in the confined concrete, concentrations of cracks and the slips between the concrete and the two tubes; these are issues to be accounted for in the development of a more accurate model in the future.

DOI: 10.1061/(ASCE)1090-0268(2006)10:5(443)

CE Database subject headings: Hybrid members; Tubular members; Beams; Flexural behavior; FRP; Steel; Concrete.

Introduction

In recent years, fiber-reinforced polymer (FRP) composites have found increasingly wide applications in civil engineering because of their well-known advantages such as their high strength-to-weight ratios and good corrosion resistance. Apart from their applications in the retrofit of structures (Teng et al. 2002), efforts are also being made around the world to explore the use of FRP composites in new construction. Current research addresses not only the performance of structures made of FRP alone (i.e., all-FRP structures) but also structures made of FRP in combination with other materials (i.e., hybrid FRP structures).

Double-skin tubular columns (DSTCs) are a column form that appears to have been first reported in late 1980s (Shakir-Khalil and Illouli 1987). A DSTC consists of two concentric steel tubes with concrete in between them. Since the late 1980s, much research has been conducted on these columns (Shakir-Khalil 1991; Wei et al. 1995; Han et al. 1995; Yagishita et al. 2000; Zhao et al. 2002; Tao et al. 2003). Compared with a conventional concrete-filled steel tubular column, i.e., a single steel tube completely filled with concrete, the inner void in a DSTC reduces the column weight without significantly affecting the flexural rigidity of the section and allows the easy passage of service ducts. The replacement of the steel tubes in a DSTC by FRP tubes has recently been explored by Fam and Rizkalla (2001).

The third author (Teng et al. 2004; Teng et al. 2005) has recently proposed a new type of hybrid FRP-concrete-steel member consisting of a steel tube inside, an FRP tube outside, and concrete in between (Fig. 1). The two tubes can be either rectangular or circular and can be placed concentrically or eccentrically (Fig. 1), with the eccentric placement of the inner steel tube being particularly attractive when the member is employed as a beam

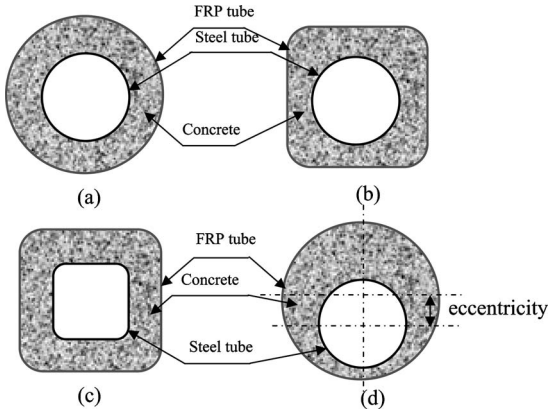

Fig. 1. Typical sections of double-skin tubular members

[1]Ph.D. Student, Dept. of Civil and Structural Engineering, The Hong Kong Polytechnic Univ., Hong Kong, China.

[2]Associate Professor, Dept. of Civil and Structural Engineering, The Hong Kong Polytechnic Univ., Hong Kong, China.

[3]Chair Professor of Structural Engineering, Dept. of Civil and Structural Engineering, The Hong Kong Polytechnic Univ., Hong Kong, China.

[4]Professor, Dept. of Civil Engineering, Zhejiang Univ., Hangzhou 310027, China.

[5]Associate Professor, Dept. of Civil and Structural Engineering, The Hong Kong Polytechnic Univ., Hong Kong, China.

Note. Discussion open until March 1, 2007. Separate discussions must be submitted for individual papers. To extend the closing date by one month, a written request must be filed with the ASCE Managing Editor. The manuscript for this paper was submitted for review and possible publication on October 28, 2005; approved on January 12, 2006. This paper is part of the ***Journal of Composites for Construction***, Vol. 10, No. 5, October 1, 2006. ©ASCE, ISSN 1090-0268/2006/5-443–452/$25.00.

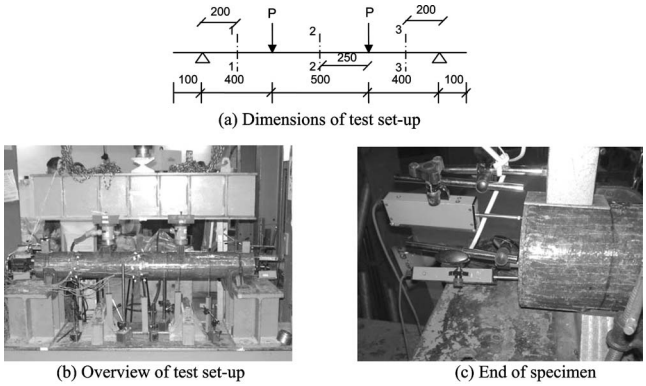

Fig. 2. Test setup

dominated by gravity loading (e.g., simply supported bridge girders). The fibers in the fiber-reinforced polymer (FRP) tube are solely or predominantly oriented in the hoop direction as the FRP tube is intended to confine the concrete and enhance the shear resistance, and the inner void may be filled with concrete if desired. This new form of hybrid members is an attempt to combine the advantages of all three constituent materials and those of the structural form of DSTCs, so as to achieve high-performance structural members.

The advantages of the new hybrid FRP-concrete-steel DSTCs are obvious when compared with steel-concrete DSTCs with two steel tubes or FRP-concrete DSTCs with two FRP tubes. Compared to steel-concrete DSTCs, the advantages of the new column form include: (a) a more ductile response of concrete as it is well confined by the FRP tube, which does not buckle; (b) no need for fire protection of the outer tube as the outer tube is required only as a form during construction and as a confining device and additional shear reinforcement during earthquakes; (c) no need for corrosion protection as the steel tube inside is well protected by the concrete and the FRP tube. Compared to FRP-concrete DSTCs, the advantages of the new column form include: (a) ability to support construction loading through the use of the inner steel tube; (b) ease of connection to beams thanks to the presence of the inner steel tube; (c) savings in fire protection cost as the outer tube is required only as a form during construction and as a confining device and additional shear reinforcement during earthquakes; (d) better confinement of concrete as a result of the increased rigidity of the inner tube. Similarly, the new column form also has significant advantages over other types of composite/hybrid columns, including concrete-filled steel tubes, concrete-filled FRP tubes, and concrete-encased steel columns, in many applications.

This paper is concerned with the flexural behavior of these new hybrid FRP-concrete-steel double-skin tubular structural members. Because columns are normally subjected to combined axial and lateral loads, their flexural behavior is important within the overall picture of the beam-column behavior of these new hybrid members. Furthermore, such hybrid sections with an eccentric inner steel tube are particularly suitable for use in beams; flexural behavior is the most important structural aspect of beams. Teng et al. (2005) presented the test results of three hybrid beam specimens in an initial assessment of the flexural behavior of such hybrid beams, which showed that these hybrid beams are highly ductile. This paper presents the first systematic study on the flexural behavior of these hybrid members in which two series of four-point bending tests (14 beam specimens) were conducted.

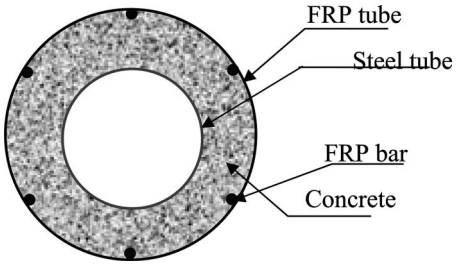

Fig. 3. Cross-section of specimens with FRP bars

Results from theoretical modeling are also presented and compared with the test results. For simplicity, the test specimens are referred to as beams hereafter, although the section form with a concentric inner tube is more suitable for columns.

Bending Tests

Test Specimens

In total, two series of four-point bending tests on hybrid FRP-concrete-steel DSTBs were conducted (Fig. 2). The specimens all had an overall length of 1,500 mm, an outer diameter of 152.5 mm, and an inner void with a diameter of about 69 mm. The first test series included eight specimens of axis-symmetric configuration (i.e., the outer FRP tube was concentric with the inner steel tube). Two of them were additionally reinforced with six 6 mm diameter longitudinal deformed FRP bars in contact with the inner surface of the FRP tube and evenly spaced around the circumference (Fig. 3). These FRP bars were intended to increase the initial flexural stiffness of the beam and to delay the development of cracks in the beam.

The second test series included six specimens in which the inner steel tube was eccentrically placed, shifted toward the tension zone of the beam section to improve the bending rigidity of the section [Fig. 1(d)]. The details of all specimens are summarized in Table 1. In this table, the steel tube eccentricity is given as the distance from the centre of the steel tube to the center of the concrete section, and D_o and t are the outer diameter and the thickness of the steel tube, respectively. The variables studied include the concrete strength (from 26.1 to 38.2 MPa), the thickness of the FRP tube (1 ply and 2 plies), the thickness of the steel tube (from 2.7 to 4.3 mm), the provision of FRP bars (6 bars), and the eccentricity of the steel tube (18.2 and 32.2 mm). It should be noted that the two steel tube eccentricities were initially designed to correspond to 20 and 0 mm concrete covers on the tension side of the section, respectively. While a 20 mm cover was achieved without difficulty, producing specimens in which the steel tube touched the FRP tube was difficult. Instead, the measured concrete covers of Specimens B-E0-32, B-E1-32 and B-E2-32 were 4.5, 5.5, and 6.5 mm, respectively. As a result, a steel tube eccentricity of 32.2 mm (or 6 mm concrete cover) was adopted as the average value for the latter two specimens in making the theoretical predictions of these two specimens. Specimen naming followed the following convention: Each name starts with the letter "B" to indicate that it is a beam specimen. "B" is followed by a letter (from "A" to "E") that represents one of the five types of steel tubes used, and that letter is followed by a number that defines the number of plies of the FRP tube. For two of the specimens in Series I, the letter "F" is added at the end to indicate the inclusion of FRP bars as additional longitudinal reinforce-

J. Compos. Constr. 2006.10:443-452.

Table 1. Details of Specimens and Measured Load Capacities

Specimen		FRP tube	Steel tube eccentricity (mm)	FRP bars	Steel tube D_o (mm)	Steel tube t (mm)	Steel tube E (MPa)	Steel tube f_y (MPa)	Steel tube f_u (MPa)	Concrete cylinder strength f_{co} (MPa)	Ultimate load P (kN)
	B-A1	1 ply	No	No	76.1	2.7	201.5	381.5	421.5	38.2	27.26
	B-A2	2 plies	No	No	76.1	2.7	201.5	381.5	421.5	38.2	27.44
	B-B1	1 ply	No	No	76.1	3.2	207.3	352.7	380.4	38.2	25.09
Series	B-B2	2 plies	No	No	76.1	3.2	207.3	352.7	380.4	35.5	26.48
One	B-C1	1 ply	No	No	76.1	4.3	197.8[a]	416.4[b]	478.6	35.5	39.36
	B-C2	2 plies	No	No	76.1	4.3	197.8[a]	416.4[b]	478.6	35.5	38.41
	B-D1-F	1 ply	No	Yes	76.1	3.5	198.7	406.2	475.5	27.8	46.28
	B-D2-F	2 plies	No	Yes	76.1	3.5	198.7	406.2	475.5	27.8	48.91
	B-E0-18	No	18.2	No	76.1	3.5	208.6[a]	340.3[b]	444.5	33.4	28.90
	B-E1-18	1 ply	18.2	No	76.1	3.5	208.6[a]	340.3[b]	444.5	33.4	35.39
Series	B-E2-18	2 plies	18.2	No	76.1	3.5	208.6[a]	340.3[b]	444.5	33.4	38.11
Two	B-E0-32	No	32.2	No	76.1	3.5	208.6[a]	340.3[b]	444.5	26.1	27.11
	B-E1-32	1 ply	32.2	No	76.1	3.5	208.6[a]	340.3[b]	444.5	26.1	36.49
	B-E2-32	2 plies	32.2	No	76.1	3.5	208.6[a]	340.3[b]	444.5	26.1	42.01

[a]Initial elastic modulus.

[b]0.2% proof stress.

ment. For Series II specimens, a two-digit number is added at the end to define the eccentricity of the steel tube. For example, Specimen B-E2-32 had a type E steel tube and a two-ply FRP tube, with the center of the former being at 32.2 mm from that of the latter.

Material Properties

Tensile tests on three steel coupons were conducted for each type of steel tube. The coupons were cut along the longitudinal direction from a steel tube of the same type and were tested following BS 18 (1987). The average experimental values of the elastic modulus (E), yield strength (f_y), and tensile strength (f_u) for each type of steel tubes are listed in Table 1. Four tensile tests for the FRP bars were also conducted basically following ACI 440.3R (2004), with two of the specimens failing near the ends and the other two failing away from the ends. The average elastics modulus from the 4 specimens is 54.5 GPa, while the average tensile strength from the two specimens in which failure occurred away from the ends is 951.7 MPa. The elastic modulus is the more important parameter for the subsequent interpretation of the test results, as the rupture strains of FRP bars in the beam specimens were measured using strain gauges. Tensile tests showed that the GFRP for making the FRP tubes had an average strength of 1,825.5 MPa, an average Young's modulus of 80.1 GPa, and an average rupture strain of 0.0228. These results were determined from tensile tests conducted following the ASTM standard (ASTM D3039 2000) on six coupons and calculated using a nominal thickness 0.17 mm per ply. These properties are for the hoop direction of the FRP tubes where the FRP fibers were oriented in the hoop direction only. Three concrete cylinders (152.5 mm $\times$ 305 mm) were cast for each batch of concrete to determine the compressive strength of each batch. The mean concrete cylinder strength (f_{co}) for each batch is also given in Table 1.

Preparation of Specimens

The preparation process of the DSTC specimens included the following steps: (1) fabrication of the formwork (Fig. 4), which consisted of a PVC tube outside, a steel tube inside, and FRP bars (for some of the specimens); (2) concrete casting; and then (3) removal of the PVC form and wet-layup formation of the FRP tube on the hardened concrete (Fig. 5). For Specimens B-D1-F and B-D2-F, the FRP bars were attached to the inner surface of the outer PVC tube at several points along their length using a sealant.

It should be noted that the FRP tube was formed by wrapping resin-impregnated fiber sheets on hardened concrete, as is done in

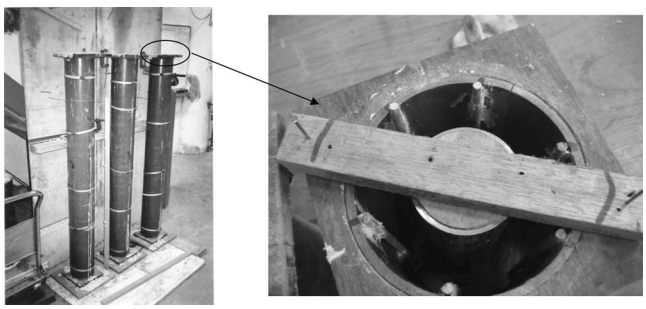

Fig. 4. Formwork for casting concrete

Fig. 5. Fabrication of FRP tube

J. Compos. Constr. 2006.10:443-452.

retrofit applications; the concrete was not cast into a prefabricated FRP tube. The wrapping process was used as prefabricated FRP tubes with fibers oriented mainly in the hoop direction were not readily available to the authors. Previous research by Shahawy et al. (2000) indicates little difference between the two methods of forming the FRP tube in terms of the performance of the hybrid column.

Test Setup and Instrumentation

The test setup is shown in Fig. 2. Except for the two specimens without an outer FRP tube (Specimens B-E0-18 and B-E0-32), sixteen strain rosettes were installed, with 8 strain rosettes evenly distributed around the circumference of the FRP tube at each of Sections 1 and 2 [Fig. 2(a)]. For those specimens with FRP bars, six additional unidirectional strain gauges (one for each bar) were installed on the FRP bars within the pure bending region. Five displacement transducers were provided at Sections 1, 2, and 3 [Fig. 2(a)] and the two loading sections [Fig. 2(b)] to measure deflections, while two other displacement transducers were provided at each end of the specimen to measure the slips between the concrete and the steel tube and between the concrete and the FRP tube, respectively [Fig. 2(c)].

For the two specimens without an FRP tube, five unidirectional strain gauges were attached on the concrete surface at different heights of the mid-span section. The provision of displacement transducers differed in that only one displacement transducer was needed at each end to monitor the slip between the concrete and the steel tube. At each loading point, a load cell was used to measure the applied load P. The test data were collected by a data logger.

Test Results, Observations, and Discussions

General Observations

The load-deflection curves are shown in Fig. 6, where the load P represents the average load recorded by the two load cells. It is clear that, except for B-A1 and B-E2-32, the beam specimens without FRP bars exhibited a smooth load-deflection curve with large deflection ductility, with the mid-span deflection exceeding 1/15 span at a less than 10% reduction in the load-carrying capacity. During the tests of B-A1 and B-E2-32, there was a sudden load drop accompanied by a loud noise, after which, however, the specimens could be reloaded to exceed the original load level.

The two specimens with FRP bars (B-D1-F and B-D2-F) also experienced sudden load drops during the tests. These load drops, which were caused by the rupture of the FRP bars, were relatively small (about 19% of the peak load) and could not be subsequently recovered. After these load drops, the specimens could still sustain an almost constant load with increasing deformation.

The tests of the specimens with an FRP tube but without FRP bars were eventually terminated because of the headroom limitation of the loading frame. For the two specimens without an FRP tube, the test was terminated when many large cracks were found on the beam (because there was no FRP tube reinforcing the beam outside) and the whole loading system became somewhat unstable. For the two specimens with FRP bars, the test was terminated when a major localized crack made the beam increasingly more asymmetric and unstable. Specimens B-B1, B-D1-F and B-E0-18 after the tests are shown in Fig. 7 to illustrate the typical deformation and crack patterns.

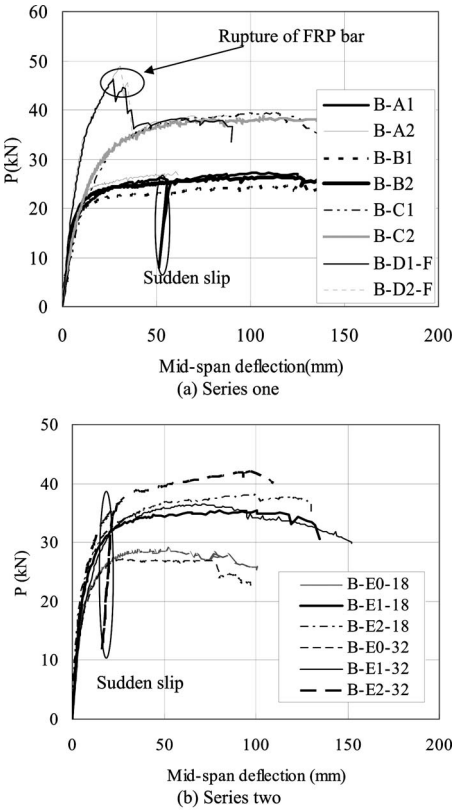

Fig. 6. Mid-span load-deflection curves

Development of Cracks

During the tests, initial flexural cracks were found in the early stage of loading. For the DSTB specimens, these initial cracks were revealed by white patches on the FRP tube caused by resin damage created by cracks in the concrete behind the tube. The initiation of cracks can also be identified from the readings of strain gauges. Fig. 8 shows two typical compressive-tensile strain curves for two specimens, in which the compressive and tensile strains are from two strain gauges located at the top and bottom of the mid-span, respectively. In both cases, the relationship between the two strains is initially linear, but after the tensile strain reaches about 0.00013, the tensile strain in Specimen B-C1 increases much more rapidly than before, while the tensile strain in Specimen B-B1 remains almost constant despite large increases of the compressive strain. This is because tensile cracks occurred within the gauge length of the strain gauge in the former case but outside the gauge length in the latter case. The end of the initial linear relationship corresponds to the occurrence of tensile cracks in the beam, which took place at about 15% of the peak load for those specimens without FRP bars and at about 20% of the peak load for those with FRP bars.

Further load increments caused new cracks and extension of existing cracks. At the end of each test, the mid-span deflection exceeded 1/15 of the span and wide cracks were found in the specimen. For the specimens with an outer FRP tube but without FRP bars, two major vertical cracks always formed right below or very close to the two load positions, and other less prominent vertical cracks were randomly distributed within and outside the pure-bending region of the specimen [Fig. 7(a)]. Inclined shear cracks were found together with flexural cracks along the specimens without an outer FRP tube [Fig. 7(c)]. For the specimens with FRP bars, no obvious cracks were found on the surface of

J. Compos. Constr. 2006.10:443-452.

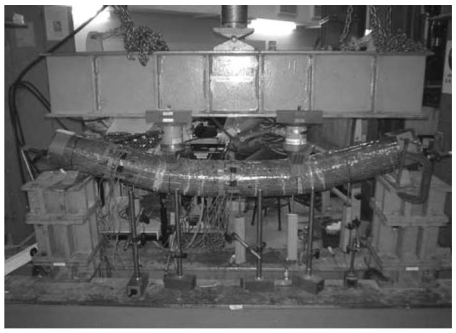

(a) Specimen B-B1

(b) Specimen B-D1-F

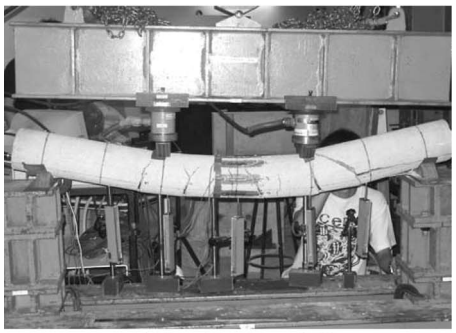

(c) Specimen B-E0-18

Fig. 7. Specimens after testing

the FRP tube before the peak load, but some visible white patches indicated the appearance of cracks in the concrete behind. After the attainment of the peak load (at a mid-span deflection of about 1/50 of the span) at the rupture of the FRP bar at the bottom of the beam, a major crack opened up at the location of rupture of the FRP bar within the pure bending region [Fig. 7(b)].

Effect of the FRP Tube

For the specimens in Series I, in which the two tubes (the FRP tube and the steel tube) were concentrically placed, the thickness of the FRP tube had little effect on the stiffness and the ultimate load of the DSTB (Fig. 6). However, local rupture of the FRP tube by hoop tension was found in the final stage of testing in some specimens with a one-ply FRP tube (Fig. 9) but in none of the two-ply FRP tubes. This implies that a thicker FRP tube will lead to a more ductile response. In addition, specimens with an FRP tube can be expected to perform better than those without an FRP tube because of the confinement to concrete and the shear resistance provided by the FRP tube.

For the specimens in Series II, which had an eccentrically placed steel tube, the one-ply FRP tube enhanced the ultimate load by over 20% for both steel tube eccentricities. A thicker FRP

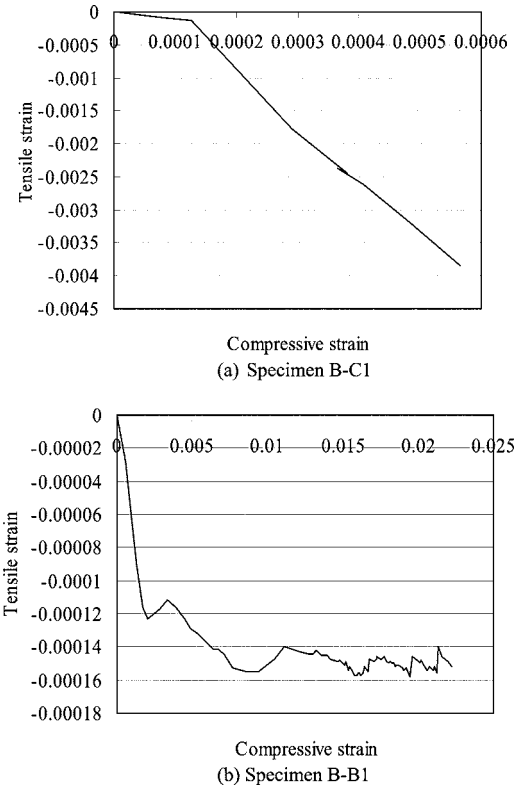

Fig. 8. Ultimate compressive-tensile strain curves

tube also helped increase the ultimate load and the ductility; local FRP rupture was again found in both specimens with a one-ply FRP tube in the final stage of testing. Indeed, for Specimens B-E1-18 and B-E1-32, the rupture of the FRP tube caused the load to begin to drop in the final stage [Fig. 6(b)]. In addition, shear cracks were found in the two specimens without an FRP tube [Fig. 7(c)], but not in the other specimens with an FRP tube [Fig. 7(a and b)]. These cracks are at least partially responsible for the poorer performance of the specimens without an FRP tube. The FRP tube clearly enhanced the shear resistance of the specimens. The shear resistance offered by the FRP tube is also confirmed by the development of significant hoop tensile strains (over 0.1%) at some locations (probably at the location of the

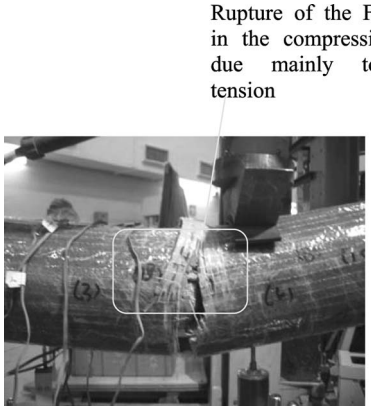

Fig. 9. Specimen B-D1-F after testing

J. Compos. Constr. 2006.10:443-452.

shear cracks in the concrete) in the lower part of the FRP tube as revealed by strain measurements made at Section 1 of the specimen [Fig. 2(a)].

FRP Confinement of Concrete

As there were only hoop fibers in the FRP tubes, their axial stiffness and strength were insignificant. The contribution of the FRP tube to the flexural behavior of a DSTB was mainly through the provision of confinement to the concrete. Axial compressive tests (Teng et al. 2005) have shown that the confinement of the concrete provided by the FRP tube in such a double-skin section can improve the ductility or both the ductility and the strength of the concrete, depending on the thickness of the FRP tube. The benefit of confinement was also present in the test beams with an FRP tube (Fig. 6 and Table 1).

The test results from Series I indicate that the thickness of the FRP tube affected the ultimate load little. This observation may mean that in these test beams, the behavior of the concrete confined by a one-ply FRP tube did not differ significantly from that of the concrete confined by a two-ply FRP tube, which differs from the conclusion drawn from the axial compression test results on closely similar DSTC sections (Teng et al. 2005). In the axial compression tests, the two-ply tube led to a significantly higher ultimate load and better ductility than those obtained for a one-ply tube. This difference in the effect of confinement between axial compression and flexural specimens may be because: (1) the area of the compressive region of concrete is much smaller (less than half of the section) in the flexural specimens, so their ultimate loads are much less sensitive to the concrete strength; and/or (2) the existence of a strain gradient over the beam section reduces the confinement effect. Previous experimental work by other researchers on concrete-filled FRP tubes has shown that the effect of confinement on concrete is less significant for beams than for columns (Fam and Rizkalla 2002; Mirmiran et al. 1999).

The test results of specimens of series II clearly indicate the benefit of a thicker FRP tube. The ultimate load of Specimen B-E2-18 is 7.69% higher than that of Specimen B-E1-18, while the ultimate load of Specimen B-E2-32 is 15.1% higher than that of Specimen B-E1-32. The larger difference between the two B-E-32 specimens may be because (1) there was more concrete in the compressive region of the B-E-32 sections with a steel tube eccentricity of 32.2 mm than the B-E-18 sections with a steel tube eccentricity of 18.2 mm, so more benefit was derived from the FRP confinement; and/or (2) the concrete in the B-E-32 specimens had a lower unconfined strength (26.1 MPa) (Table 1), which made the effect of FRP confinement more significant in terms of strength increases relative to the unconfined strength, as has been shown by existing research (Teng and Lam 2004).

For the specimens in Series I, although the thickness of the FRP tube had little effect on the ultimate load, it did lead to a clear difference in the axial strain-hoop strain behavior (at the top compressive fiber). Fig. 10 shows two axial strain-hoop strain curves for Specimens B-C1 and B-C2 with a one-ply FRP tube and a two-ply FRP tube, respectively. Both curves indicate that as the axial strain increases, the rate of increase in the hoop strain initially increases and then remains more or less constant. In the later stage of loading, at the same axial compressive strain, the hoop strain for the one-ply tube is about twice that for the two-ply tube, so the two tubes provide about the same amount of confinement as their thicknesses were different. For instance, at an axial compressive strain of 0.008, the hoop tensile strain is 0.0052 for B-C1 and 0.0029 for B-C2. This greater demand on the hoop deformation of the one-ply tube explains why some of the one-ply

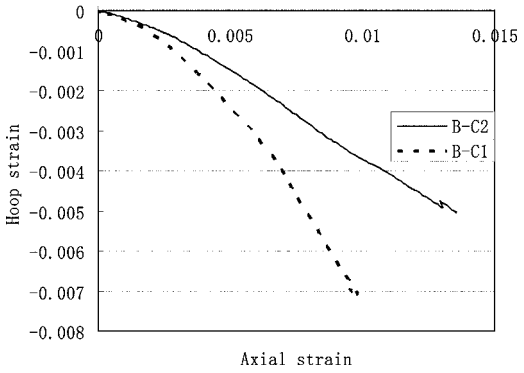

Fig. 10. Axial-hoop strain behavior

FRP tubes but none of the two-ply FRP tubes failed by rupture and why DSTBs with a thicker FRP tube can be expected to exhibit greater ductility.

Slips between the Concrete and the Tubes

The slip between the concrete and the FRP tube was insignificant (almost zero) in all cases except for B-E2-32 because of the small axial stiffness of the FRP tube. The slip between the concrete and the steel tube, however, was much larger (about 10 mm at the end of test for most of the specimens). The steel tube-to-concrete slip gradually increased with the mid-span deflection except for specimen B-A1.

During the test of Specimen B-A1, there was a sudden load drop accompanied by a loud noise at a load $P=26.1$ kN with a mid-span deflection of 54.1 mm. The LVDT readings at the two ends of the specimen revealed that there was a sudden increase in the slip between the concrete and the steel tube at the onset of this sudden load drop. It is believed that this sudden slip increase was caused by at least a partial loss of the composite action between the concrete and the steel tube. This phenomenon indicates that an improvement to the bond between the concrete and the steel tube in such DSTBs may be needed.

During the test of Specimen B-E2-32, there was also a sudden load drop with a loud noise at a load $P=35.4$ kN with a mid-span deflection of 21.5 mm. The associated slip between the concrete and the FRP tube was about 0.65 mm. This suggests that the bond between the concrete and the FRP tube in such DSTBs may also need improvement, particularly if the FRP tube possesses significant axial stiffness.

It is evident from the test observations that improvements to the bond resistance at both interfaces are desirable. Roughening treatments on the tubes and the use of mechanical connectors are possible alternatives to achieve enhanced interfacial bond resistance.

Effect of FRP Bars

Two of the beams (B-D1-F and B-D2-F) had FRP bars as additional longitudinal reinforcement. These FRP bars were provided to avoid the early development of cracks in the tensile concrete. The FRP bars enhanced both the stiffness and the ultimate load of the beam. These beams displayed almost linear load-deflection behavior up to a mid-span deflection of about 1/100 of the span (or about 80% of the ultimate load). Afterward, the stiffness of the beam reduced continuously while the load kept increasing until the ultimate load was reached at a mid-span deflection of about 1/50 of the span. No obvious cracks were found on the surface of the FRP tube before the peak load, as stated earlier. At the ulti-

J. Compos. Constr. 2006.10:443-452.

mate load, a sudden and large noise was heard. The load dropped abruptly to a lower level, a major crack opened up, and the midspan deflection increased significantly. This failure was caused by the rupture of the FRP bar at the bottom of the beam, which was subjected to the largest tensile strain. After this large reduction in load, the specimen continued to sustain a considerable load in a ductile manner. Fig. 6(a) shows a comparison of the load-deflection responses of specimens with or without FRP bars. It is clear that the provision of FRP bars provides an effective means to enhance the flexural stiffness and the ultimate load of the member and to suppress early cracking.

Effect of the Steel Tube

In the present hybrid members, the steel tube is the sole longitudinal reinforcement, unless FRP bars are also provided. The steel tube thus plays a very important role in resisting loading and ensuring a ductile response. With all other parameters being the same, a thicker steel tube leads to a higher ultimate load, as can be seen by comparing the results for specimens with a 4.3 mm thick steel tube (Specimens B-C1 and B-C2) to those for specimens with a 2.7 mm or 3.2 mm thick steel tube (Specimens B-A1 and B-A2 and Specimens B-B1 and B-B2) [Fig. 6(a)]. For the two groups of specimens with steel tube thicknesses of 2.7 mm and 3.2 mm, respectively, the small benefit of the slightly thicker tube was offset by a lower yield stress, so the effect of steel tube thickness is unclear in Fig. 6(a).

For the hybrid section to be employed in a beam, the flexural stiffness and strength of the beam can be enhanced by shifting the steel tube toward the tension side, which also leaves more concrete in the compression zone. The specimens in Series II were tested to demonstrate the performance of DSTBs with an eccentrically placed steel tube. The test results show that the ultimate load of Specimen B-E1-18 is about 40% higher than that of Specimen B-B1 (Table 1), although the two had similar steel tubes, FRP tubes, and concrete. Specimen B-E1-18 also displayed a higher flexural stiffness than did Specimen B-B1 (Fig. 6). Similar conclusions can be drawn by comparing the results of Specimens B-E2-18 with B-B2. It can also be found that the ultimate loads of Specimens B-E1-32 and B-E2-32 are respectively higher than those of Specimens B-E1-18 and B-E2-18 (3.1% for one-ply tubes and 10.23% for two-ply tubes), although the unconfined concrete strength of the former two specimens is much lower (28%) than that of the latter two specimens. This is because the former two specimens had a larger steel tube eccentricity. It may also be noted that the difference in the ultimate load is larger between the two specimens with a two-ply tube; this suggests that the effect of FRP confinement on the concrete is more significant for these specimens.

Theoretical Analysis

Analysis Model

A traditional section analysis of the so-called fiber element approach was developed for the present DSTBs based on the plane section assumption and the assumption that all FRP bars become ineffective once rupture of the most highly stressed FRP bar occurs. The analytical procedure involves the determination of the position of the neural axis for a given strain of the extreme compression fiber by force equilibrium and the evaluation of the bending moment by integrating the contributions of stresses over the section.

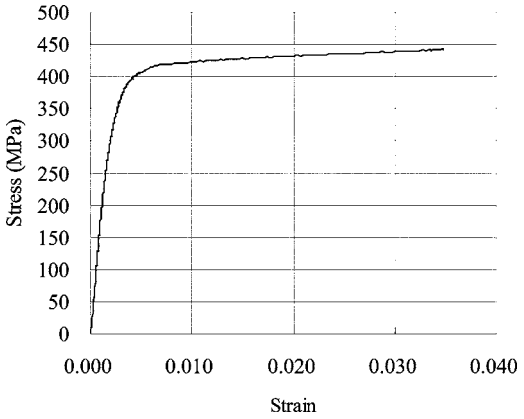

Fig. 11. Typical stress-strain curve of steel tube in B-C1

The stress-strain behavior of the steel tubes was modeled based on their tensile test results. For specimens in Series I except Specimens B-C1 and B-C2, an elastic-perfectly plastic stress-strain curve was adopted with the elastic modulus and the yield stress for each type of steel tube as given in Table 1. For Specimens B-C1 and B-C2 and the specimens in Series II, the experimental stress-strain curves did not show an elastic-perfectly plastic shape. A typical curve for the steel of Specimens B-C1 and B-C2 is shown in Fig. 11. For these specimens, the stress-strain curve for each type of steel tube was modeled by representing the average experimental stress-strain curve with a large number of data points.

The concrete was assumed to possess the same initial elastic modulus in both tension and compression. Tensile cracking was assumed to occur at a tensile strain of 130 $\mu\varepsilon$ based on test observations [e.g., Fig. 8(b)], and the concrete was assumed to resist no tensile stresses after cracking. As the behavior of beams with a one-ply tube differed from that of beams with a two-ply tube only slightly (Fig. 6), the same stress-strain curve was assumed for concrete in compression for both cases. Based on the results from axial compression tests on DSTCs with a one-ply FRP tube (Teng et al. 2005), the following equations were adopted to model the compressive stress-strain curve of the confined concrete in the present DSTBs:

$$\sigma_c = f'_{co}\left[\frac{2\varepsilon_c}{\varepsilon_{co}} - \left(\frac{\varepsilon_c}{\varepsilon_{co}}\right)^2\right] \quad \text{when } \varepsilon_c \leq \varepsilon_{co}$$

$$\sigma_c = f'_{co} \quad \text{when } \varepsilon_c > \varepsilon_{co}$$

in which σ_c and ε_c=the stress and strain of concrete, respectively, whereas f'_{co} and ε_{co}=the unconfined concrete cylinder strength and the corresponding strain, respectively. For each specimen, the longitudinal strain at the extreme compression fiber of its FRP tube, reached at the end of test, was taken as the ultimate point of the stress-strain curve of its confined concrete.

A linear stress-strain curve was adopted for FRP bars based on the tensile test results. The contribution of the outer FRP tube in the longitudinal direction was neglected as it did not have longitudinal fibers.

Load-Strain Curves

Specimen without FRP Bars

Figs. 12(a–f) show comparisons of predicted and experimental load-strain curves for Specimens B-C1, B-C2, B-E1-18, B-E2-18,

J. Compos. Constr. 2006.10:443-452.

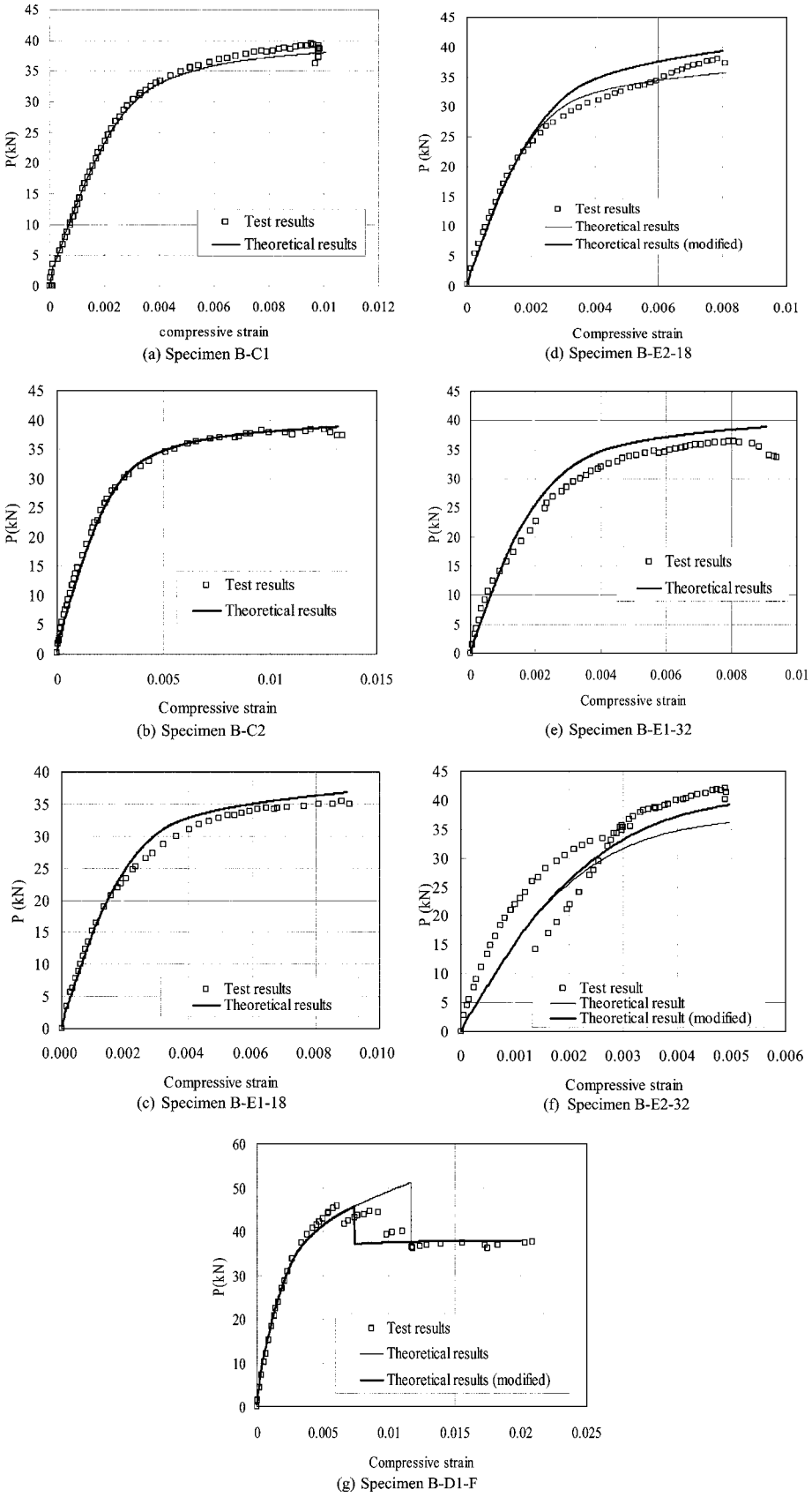

Fig. 12. Comparison of load-compressive strain curves

J. Compos. Constr. 2006.10:443-452.

B-E1-32, and B-E2-32, respectively. The strain values shown are those of the extreme compressive fiber at the mid-span. These specimens cover different section configurations, different steel tube eccentricities, and different FRP tube thicknesses.

It is evident that the theoretical results agree well with the test results for all specimens with a one-ply FRP tube (B-C1, B-E1-18, and B-E1-32), and Specimen B-C2, which had a two-ply FRP tube and a concentric steel tube, but underestimate the test results for specimens with a two-ply FRP tube and an eccentric steel tube (Specimens B-E2-18 and B-E2-32). This error for the latter case is caused by the use of the same compressive stress-strain curve for the confined concrete obtained from axial compression tests on specimens with a one-ply FRP tube, regardless of the thickness of the FRP tube in the DSTBs. This observation is consistent with the previous observation (Fig. 6) that while the thickness of the FRP tube had little effect on the performance of DSTB specimens with a concentric steel tube, it did affect the response of DSTB specimens with an eccentric steel tube. For the latter specimens, a stress-strain curve that reflects the effect of the FRP tube thickness more accurately is needed for more accurate predictions.

To improve the predictions, one of the two almost identical stress-strain curves obtained from axial compression tests on DSTCs with a two-ply FRP tube (Teng et al. 2004) was adopted to generate another set of results. For use in the analysis model, the compressive stress-strain curves of concrete in the DSTCs and in the present DSTBs were assumed to be the same when they were normalized by their respective unconfined concrete strength and the corresponding strain. The results predicted with this modified stress-strain curve [labeled as "theoretical results (modified)"] are also compared with the test results in Figs. 12(d and f). For both Specimens B-E2-18 and B-E2-32, the ultimate load can now be closely predicted, but significant errors remain in the predicted load-strain response. In particular, considerable errors remain for the initial part of the load-strain curve of Specimen B-E2-32 [Fig. 12(f)]. These errors may be attributed to slips between the FRP tube and the concrete that might have existed right from the beginning of loading due to the greater thickness of the FRP tube (i.e., greater axial rigidity) of Specimen B-E2-32, so that the strains recorded on the FRP tube are smaller than predictions based on the plane section assumption. Indeed, the sudden slip found during the test of this specimen, but not in other specimens, supports this explanation.

Comparisons for other specimens also found close agreement, although a more significant difference was noted for two specimens in which a crack did not develop near the mid-span strain gauge (e.g., Specimen B-B1).

Specimens with FRP Bars

Fig. 12(g) shows a comparison of load-strain curves for one of the two specimens with FRP bars. The comparison for the other specimen is similar. The theoretical load-strain curve follows the experimental curve closely but then exceeds it considerably with a significantly higher ultimate load. It was found that the rupture strain of the FRP bar in the beam tests (0.011) was much lower (about 36%) than the rupture strain obtained from tensile tests (about 0.017), which were adopted in the analysis. The degradation of rupture strain of the FRP bar in the beam tests may be the result of the presence of bending deformation in the FRP bar. This reduction in the rupture strain explains the difference between the predicted and experimental load-strain curves. An alternative prediction, in which the reduced rupture strain observed in the beam tests replaced that from the tensile tests, is also shown in Fig. 12(g) [labeled "theoretical results (modified)"]. This alternative prediction is in much closer agreement with the experimental curve.

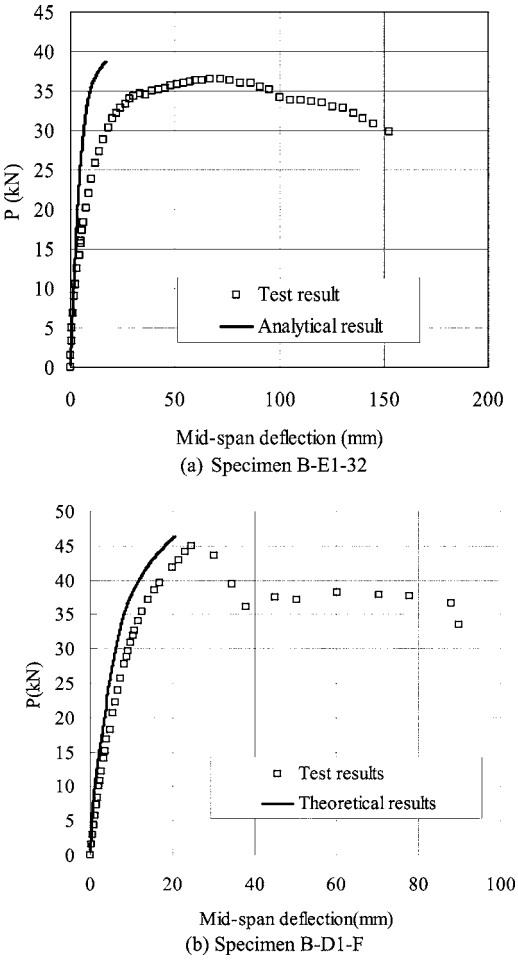

Fig. 13. Comparison of mid-span load-deflection curves

Load-Deflection Curves

The results from the section analysis can be integrated to predict the deflections of the beam. Fig. 13 shows comparisons between the experimental and the predicted mid-span load-deflection curves for Specimen B-E1-32, which had no FRP bars, and for Specimen B-D1-F, which had FRP bars. For Specimen B-E1-32, the theoretical results agree well with the test results up to a load level of about 1/3 of the ultimate load, after which the difference between the theoretical and test results becomes more significant. The differences are believed to be mainly caused by the development of wide localized cracks in the beam and slips between the concrete and the tubes, both of which were not considered in the analysis. For Specimen B-D1-F, the predicted curve ends at the rupture of the FRP bar at the bottom, as the accuracy of the section analysis further deteriorates due to the appearance of a wide crack at the location of FRP bar rupture immediately afterward. It can be seen from Fig. 13(b) that the prediction is more accurate than that for Specimen B-E1-32. This is consistent with the test observation that no large cracks were found in Specimen B-D1-F before the rupture of the bottom FRP bar. Some small

J. Compos. Constr. 2006.10:443-452.

differences between the test and predicted results still exist; these may be attributed to some slips between the concrete and the tubes (particularly the steel tube).

Conclusions

This paper has presented and interpreted the results of two Series of 4-point bending tests on hybrid DSTBs. A DSTB is composed of a steel inner tube, an FRP outer tube, and a concrete infill between the two tubes. The main parameters examined in this study include the section configuration and the thicknesses of the steel tube and the FRP tube. A simple theoretical model based on the plane section assumption and the fiber element approach was also developed and employed to predict the responses of the test beams. Based on the test results and the comparisons with theoretical predictions, the following conclusions can be drawn:

1. The hybrid DSTBs possess a very ductile response. The FRP tube confines the concrete and provides additional shear resistance. The steel tube provides ductile longitudinal reinforcement.
2. A DSTB with an eccentric steel tube benefits more significantly from the outer FRP tube than a corresponding DSTB with a concentric steel tube because in the former a larger amount of concrete is in the compression zone.
3. Significant slips between the concrete and the two tubes, particularly the steel tube, and associated load fluctuations may occur. Improvements to the bond resistance at both interfaces are desirable.
4. The flexural response of a DSTB, including the flexural stiffness, the ultimate load, and cracking, can be substantially improved by shifting the inner steel tube toward the tension region or providing FRP bars as additional longitudinal reinforcement.
5. The effect of FRP confinement on concrete in beam specimens is less significant than that in column specimens of identical sections, because of the existence of a strain gradient and a relatively small concrete compression zone.
6. The predictions from the theoretical model are in reasonably close agreement with the test results. Differences arise from factors not considered in the theoretical model, including the concentrations of cracks and the slips between the concrete and the two tubes. The development of a more accurate model should take these factors into account and use a more accurate stress-strain model for the confined concrete in DSTBs. Furthermore, a method for predicting the ultimate strain for the stress-strain equation needs to be established.

Acknowledgments

The work presented in this paper has received financial support from the Hong Kong Polytechnic University through a research studentship to the first author and the Young Professorship Scheme (Project No: 1ZE-06) and through a Distinguished Young Scholar Award of the Natural Science Foundation of China (Project No. 50329802). The authors are grateful to both organizations for their financial support.

References

ACI 440.3R. (2004). *Guide test methods for fiber-reinforced polymers (FRPs) for reinforcing or strengthening concrete structures*, ACI Committee 440, Farmington Hills, Mich.

ASTM D 3039. (2000). *Standard test method for tensile properties of polymer matrix composite materials*, ASTM Committee D30, Philadelphia.

BS 18. (1987). *Tensile testing of metals (including aerospace materials)*, British Standards Institution, London, U.K.

Fam, A. Z., and Rizkalla, S. H. (2001). "Behavior of axially loaded concrete-filled circular fiber-reinforced polymer tubes." *ACI Struct. J.*, 98(3), 280–289.

Fam, A. Z., and Rizkalla, S. H. (2002). "Flexural behavior of concrete-filled fiber-reinforced polymer circular tubes." *J. Compos. Constr.*, 6(2), 123–132.

Han, B., Xia, J., and Zhao, J. (1995). "The strength of concrete filled double-skin steel tubes under axial compression." *Journal of Shijiazhuang Railway Institute*, 8(3), 75–80.

Mirmiran, A., Shahawy, M., and Samaan, M. (1999). "Strength and ductility of hybrid FRP-concrete beam-columns." *J. Struct. Eng.*, 125(10), 1085–1093.

Shahawy, M., Mirmiran, A., and Beitelman, T. (2000). "Tests and modeling of carbon-wrapped concrete columns." *Composites, Part B*, 31(6–7), 471–480.

Shakir-Khalil, H. (1991). "Composite columns of double-skinned shells." *J. Constr. Steel Res.*, 19, 133–152.

Shakir-Khalil, H., and Illouli, S. (1987). "Composite columns of concentric steel tubes." *Proc., Conf. on the Design and Construction of Non-Conventional Structures*, Vol. 1, London, pp. 73–82.

Tao, Z, Han, L. H., and Huang, H. (2003). "Concrete-filled double-skin steel tubular column with square section under eccentric loads." *China Civ. Eng. J.*, 36(2), 33–40.

Teng, J. G., Chen, J. F., Smith, S. T., and Lam, L. (2002). *FRP strengthened RC structures*, John Wiley & Sons Ltd., New York.

Teng, J. G., and Lam, L. (2004). "Behavior and modeling of FRP-confined concrete." *J. Struct. Eng.*, 130(11), 1713–1723.

Teng, J. G., Yu, T., and Wong, Y. L. (2004). "Behavior of hybrid FRP-concrete-steel double-skin tubular columns." *Proc., 2nd Int. Conf. on FRP Composites in Civil Engineering*, Adelaide, Australia, 811–818.

Teng, J. G., Yu, T., Wong, Y. L., and Dong, S. L. (2005). "Hybrid FRP-concrete-steel tubular columns: Concept and behavior." *Constr. Build. Mater.*, accepted for publication.

Wei, S., et al. (1995). "Performance of new sandwich tube under axial loading: Experiment." *J. Struct. Eng.*, 121(12), 1806–1814.

Yagishita, F., Kitoh, H., Sugimoto, M., Tanihira, T., and Sonoda, K. (2000). "Double-skin composite tubular columns subjected to cyclic horizontal force and constant axial force." *Proc., 6th ASCCS Int. Conf. on Steel-Concrete Composite Structures*, 497–503.

Zhao, X. L., Grzebieta, R., and Elchalakani, M. (2002). "Tests of concrete-filled double-skin CHS composite stub columns." *Steel Compos. Struct.*, 2(2), 129–146.

J. Compos. Constr. 2006.10:443-452.